Available online at www.sciencedirect.com
ScienceDirect
Ceramics International 34 (2008) 1543–1549
CERAMICS INTERNATIONAL
www.elsevier.com/locate/ceramint

Effect of zirconia addition on pressureless sintering of boron carbide

C. Subramanian [a,*], T.K. Roy [b], T.S.R.Ch. Murthy [a], P. Sengupta [a], G.B. Kale [a], M.V. Krishnaiah [c], A.K. Suri [a]

[a] *Materials Group, Bhabha Atomic Research Centre, Mumbai, India*
[b] *Variable Energy Cyclotron Centre, Kolkata, India*
[c] *Materials Chemistry Division, Indira Gandhi Centre for Atomic Research, Kalpakkam, India*

Received 11 September 2006; received in revised form 11 March 2007; accepted 28 April 2007
Available online 2 June 2007

Abstract

This paper presents the results of experiments on pressureless sintering of boron carbide with varying addition of zirconia (ZrO_2: 0–30 wt.%). Green pellets were densified by sintering at 2275 °C in vacuum for 60 min and characterized by measurement of density, hardness, thermal conductivity and microstructure. Samples prepared with the addition of ≥5 wt.% ZrO_2 showed higher densities in the range of 93–96% ρth, compared to 86.63% ρth for boron carbide only. Addition of ZrO_2 was found to increase the hardness of sintered samples and regardless of ZrO_2 content, the hardness values ranged between 30 and 31.5 GPa. XRD of the sintered pellets showed the presence of ZrB_2. Optical microscope as well as electron probe microanalysis (EPMA) showed the presence of two phases, grey matrix with white precipitates. EPMA analysis of second phase revealed the presence of Zirconium in this phase. Fractography of boron carbide with 25% ZrO_2 showed the failure to be by mixed fracture (transgranular and intergranular). Thermal conductivity values of the samples measured in the temperature range of 400–1000 °C were marginally higher with the addition of ZrO_2.

Keywords: C. Thermal conductivity; Boron carbide; Pressureless sintering; Additive ZrO_2

1. Introduction:

Boron carbide is an important ceramic material with high melting point (2450 °C), outstanding hardness and low specific gravity (2.52 g/cc). Knoop hardness of pressureless sintered boron carbide and hot pressed material are reported as $\sim 25.5 \pm 2.4$ GPa and $\sim 29.0 \pm 1.5$ GPa, respectively [1]. Boron carbide is used as neutron absorber owing to its high boron content, chemical stability and refractory character [2]. Other industrial uses of boron carbide are as abrasives for lapping, grinding and polishing media for hard materials and as wear-resistant components.

B_4C possesses strong bonding, low plasticity, high resistance to grain boundary sliding and low superficial tension in the solid state; all these factors make densification of powders difficult by sintering [3]. In addition, the presence of B_2O_3 on B_4C surface slows down the densification process [4].

A few of the recent publications that appeared on the sintering of B_4C with oxide additives are given below. Goldstein et al. reported that heating of B_4C–YTZP (Yttria stabilized zirconia polycrystals) mixtures to temperature of ~2000 °C yielded B_4C–ZrB_2 composites with better densification than monolithic B_4C [5]. Kim et al. have reported on the reaction sintering and mechanical properties of B_4C with addition of ZrO_2 by hot pressing and pressureless sintering [6]. Levin et al. have studied the effect of TiO_2 and Ti additions on the sintering behavior of B_4C in the temperature range of 1800–2190 °C [7]. TiO_2 reacts with B_4C to yield a two phase composite consisting of TiB_2 and sub-stiochometric B_4C_{1-x} [7,8]. Skorokhod et al. studied the mechanical properties of pressureless sintered boron carbide with in situ reaction of TiO_2 and carbon [9]. Frage studied the effect of addition of chromium oxide on sintering of boron carbide and identified the formation of reaction product CrB_2 in the sintered composite [10]. Golstein et al. reported the formation of B_4C + metal boride (TiB_2, ZrB_2, VB_2, VB, CrB_2, YB_2, YB_4, LaB_6, $LaB_6 + ZrB_2$) composites (>95% ρth) by in situ reaction of B_4C and metal oxide (TiO_2, ZrO_2, V_2O_5, Cr_2O_3, Y_2O_3, La_2O_3,

* Corresponding author. Tel.: +91 22 25593937; fax: +91 22 25505151.
E-mail address: csubra@barc.gov.in (C. Subramanian).

0272-8842/$34.00
doi:10.1016/j.ceramint.2007.04.017

$L_2O_3 + ZrO_2$) mixtures [11]. Sigl investigated the fabrication of $B_4C + TiB_2$ composite with traces of carbon by sintering a mixture of B_4C and TiC [12]. Frage et al. while studying on the effect of sintering atmosphere have noted improved densification under a combined vacuum-argon instead of nitrogen atmosphere [13].

Particle size of boron carbide powder and the sintering temperature are two most important parameters for densification by pressureless sintering. Previous work in the same laboratory reported that density of boron carbide pellets obtained to be less than 85% ρth by sintering at temperatures below 2300 °C using particles in the size range of 0.5–2.0 μm. Highest density of ∼90% ρth was obtained while sintering at a higher temperature of 2375 °C [14]. The present paper reports on pressureless sintering of boron carbide with the addition of ZrO_2 and its characterization.

2. Experimental procedure

2.1. Materials

Boron carbide powder of ∼1 μm median diameter was used in the present investigation. Preparation of such fine powders has been reported in our earlier paper [14]. Powders were characterized by chemical analysis and laser particle size analyzer. Zirconium oxide used was of reactor grade obtained from Nuclear Fuel Complex, Hyderabad. Table 1 presents the chemical analysis of boron carbide.

2.2. Procedure

To understand the interaction between B_4C and ZrO_2, thermograviometric experiment was conducted (Setaram, TAG 24) up to 2000 °C under vacuum with 5% ZrO_2 sample. For sintering studies boron carbide with ZrO_2 (0, 2.5, 5, 7.5, 10, 15, 20, 25 and 30 wt.%) powders were thoroughly mixed in a motorized mortar–pestle and then compacted under a pressure of about 280 MPa to form pellets of 10 mm diameter and 10 mm height with a green density of ∼65% ρth. These compacts were sintered at 2275 °C temperature under a dynamic vacuum of 1×10^{-2} Pa in an induction furnace for 60 min. Densities of the pellets were measured using Archimedes principle in distilled water. Sintered pellets were cut, polished up to 1 μm finish and etched [15] for microscopic observation. Selected samples were characterized by optical microscope, Cu Kα ($\lambda = 1.5404$ Å) XRD (40 kV, Philips PW1830), SEM (30 kV, Tescan) and EPMA (15 kV, Cameca SX 100). Thermal diffusivity and micro hardness were measured using laser flash thermal diffusivity meter and micro hardness tester (Future tech FM-7, Tokyo), respectively.

Table 1
Chemical analysis of boron carbide

Element	B	C	Fe	Si	Ni	Cr	O	N
Wt.%	78.00	19.05	1.11	0.45	0.08	0.02	0.5	0.2

3. Results and discussions

In the densified pellets, the amount of ZrB_2 was estimated based on the following reaction for calculation of density values.

$$2ZrO_2 + B_4C\,[3C] \rightarrow 2ZrB_2 + 4CO$$

Carbon for the above reaction was taken, as that present in boron carbide as free carbon. No extra carbon was added to the charge. The amount of carbon required for the reaction varies with the amount of ZrO_2. The sample with the highest ZrO_2 content (30 wt.%) needs 4.32 wt.% carbon for the complete conversion of ZrO_2 into ZrB_2. The sample used in our studies was a commercially available material produced by carbothermic reduction of boric acid in an Acheson furnace**.** XRD of starting boron carbide sample shows the presence of graphite (Fig. 1a).

It is well known that homogeneity range of rhombohedral boron carbide extends from $B_{10.4}C$ [8.8 at.% C] to B_4C [20 at.% C][16]. B_4C is in equilibrium with free carbon [17] and is only boundary between B_nC and $B_nC + C$ (where $4 < n < 10$) [18], synthesis of B_4C without free carbon is practically impossible. B/C ratio in stiochometric compound B_4C is 3.6, where as that of our sample is 4.09 (computed from chemical analysis), indicating the presence of boron rich phase such as $B_{13}C_2$. XRD peaks of B_4C and $B_{13}C_2$ phases are too close making the identification difficult.

3.1. Thermograviometric studies

DTG-TG graph of the $B_4C + 5\%$ ZrO_2 sample is presented in Fig. 2. DTG showed three humps, the first one below 200 °C, the second one between 1000 and 1500 °C and third one above

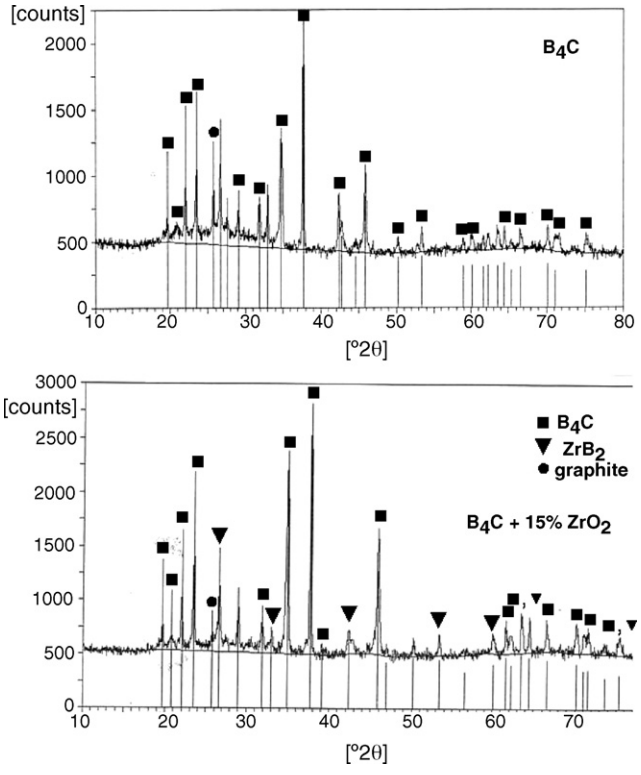

Fig. 1. XRD pattern of (a) B_4C and (b) $B_4C + 15\%$ ZrO_2 samples.

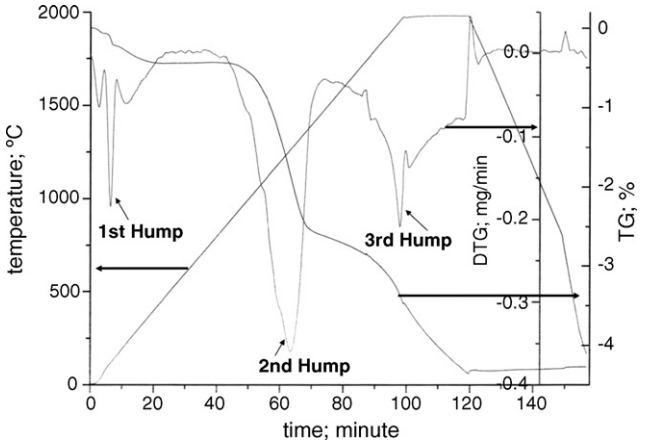

Fig. 2. TGA plot of B_4C + 5% ZrO_2 sample.

1750 °C. The nominal weight loss (<0.5%) at the start is due to evaporation of moisture and other volatiles. The total weight loss observed as 4.2% is slightly lower than the theoretical value of 4.9%. XRD of the product revealed the presence of ZrB_2 as reaction product. Kim et al. have suggested that weight loss of the samples attributed to the formation of CO and BO gas [6]. However in present study the weight loss matches with the formation of CO only. DTA studies carried by Goldstein et al. showed that solid state reactions between B_4C and ZrO_2 started at ∼1150 °C [5]. In present case the start of the reaction is seen at ∼1000 °C. This could be explained by the reason that present investigations have carried out in vacuum and not in argon atmosphere.

3.2. Density

Table 2 presents data on the densities of pressureless sintered samples with varying addition of ZrO_2 to B_4C. Pellet sintered with 0% of ZrO_2 showed a density of 86.63% ρth, which increased with the addition of ZrO_2. Theoretical density was calculated using the rule of mixture of B_4C and ZrB_2. The density obtained with 2.5 wt.% (1.1 vol.%) ZrO_2 addition was 89.56% ρth. Pellets sintered with higher amounts of ZrO_2 from 5 to 30 wt.% (2–15 vol.%) showed higher densities in the range of 93–96% ρth. Goldstein et al. obtained comparatively lower densities while sintering B_4C at 2160 °C for 60 min [5]. Upto 7% ZrO_2 addition, they have reported a density of 83% ρth and higher densities of 91 and 97.5% ρth with the addition of 15and 30 wt.% Yttria-stabilized polycrystalline tetragonal zirconia (YTZP), respectively [5]. Kim et al. also achieved only lower densification by pressureless sintering at 2175 °C with addition of ZrO_2. A high density 95%ρth was obtained with the addition of 10 vol.% (∼21 wt.%) ZrO_2 [6]. In a recent publication, Golstein et al. have stated that minimum amount of ZrO_2 needed for obtaining ∼95%ρth by sintering at 2180 °C for 2 h is 18 vol.% [11]. We have obtained higher densities probably due to higher sintering temperature.

Table 2
Density of sintered B_4C samples with variation of ZrO_2

S. no.	ZrO_2 wt.%	Measured density (g/cc)	Theoretical density (g/cc)	%ρth
1	0.0	2.1833	2.5200	86.63
2	2.5	2.2882	2.5548	89.56
3	5.0	2.4323	2.5914	93.86
4	7.5	2.4897	2.6300	94.67
5	10	2.5450	2.6706	95.30
6	15	2.6350	2.7591	95.50
7	20	2.6608	2.8585	93.08
8	25	2.8470	2.9711	95.82
9	30	2.8622	3.0997	92.34

3.3. Micro hardness

Samples of boron carbide sintered without ZrO_2 additive showed a hardness value of 27 ± 1 GPa and that with the addition of ZrO_2 a higher value in the range of 30–31.5 GPa (Fig. 3). Kim et al. reported the hardness value of 25 GPa for pressureless sintered 10 vol.% ZrO_2 sample [6]. Goldstein et al. also have reported hardness value of 30–33 GPa for fully dense B_4C–ZrB_2 composite [5].

3.4. X-ray diffraction

X-ray diffraction patterns of all the samples prepared with ZrO_2 addition showed the presence of B_4C, ZrB_2 and graphite only. X-ray pattern of pure boron carbide and sample with 15 wt.% ZrO_2 are presented in Fig. 1b. In all the samples an unknown peak is seen at 29.33°.

3.5. Microscopic examination

Microstructures of sintered boron carbide samples are given in Figs. 4 and 5. Fig. 4a presents the sample with 0% ZrO_2 with small and uniformly distributed pores, some of which are interconnected. Microstructures of B_4C with 2.5% and, 5 wt.% ZrO_2 are shown in Fig. 4(b and c). Uniform sized grains with a clear grain boundary are visible in both these samples. Closed and uniformly distributed pores (<10 μm)

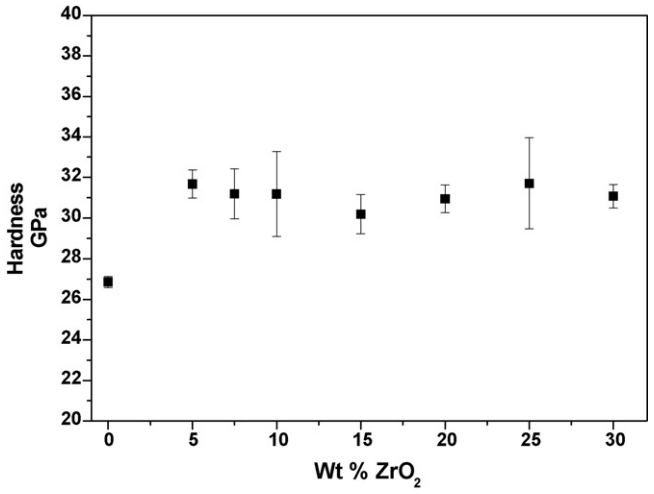

Fig. 3. Variation of hardness with ZrO_2 addition. (Line joining the points is for visual aid only).

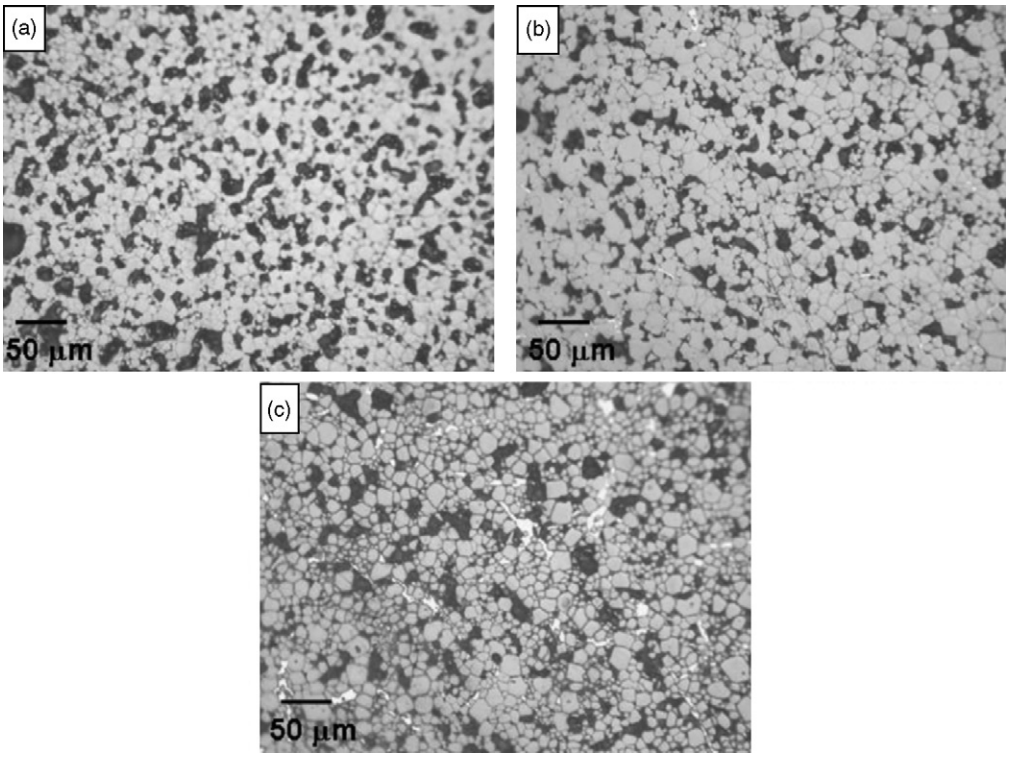

Fig. 4. Optical images of polished and etched samples (a) B_4C; (b) B_4C + 2.5 wt.% ZrO_2; and (c) B_4C + 5 wt.% ZrO_2.

and a grain growth up to 20 μm is seen. It may be mentioned here that many of the black spots appearing in the images are due to the pull out during polishing. Microstructures of the samples sintered with 10, 15, 20 and 25 wt.% ZrO_2 addition to B_4C are presented in Fig. 5(a–d). By visual examination one can see the quantity of white phase increases with the increased addition of ZrO_2. Appearance of big grains in all the cases indicated grain growth at this temperature of sintering.

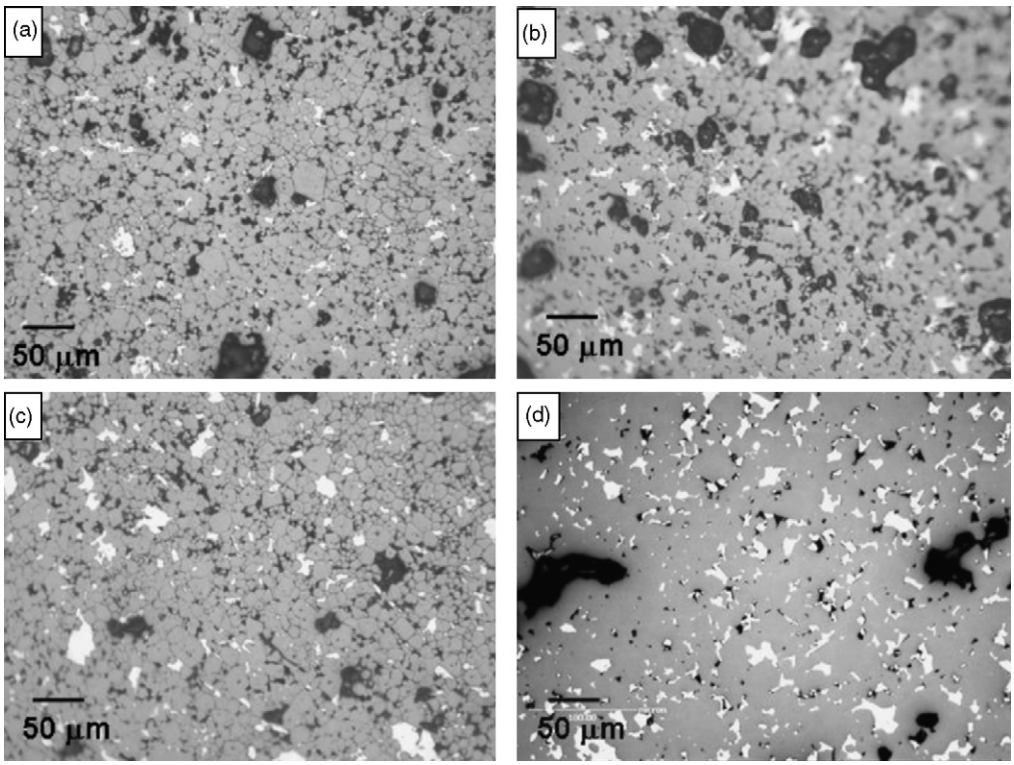

Fig. 5. Optical images of polished and etched samples (a) B_4C + 10 wt.% ZrO_2 (b) B_4C + 15 wt.% ZrO_2; (c) B_4C + 20 wt.% ZrO_2;and (d) B_4C + 25 wt.% ZrO_2 (not etched).

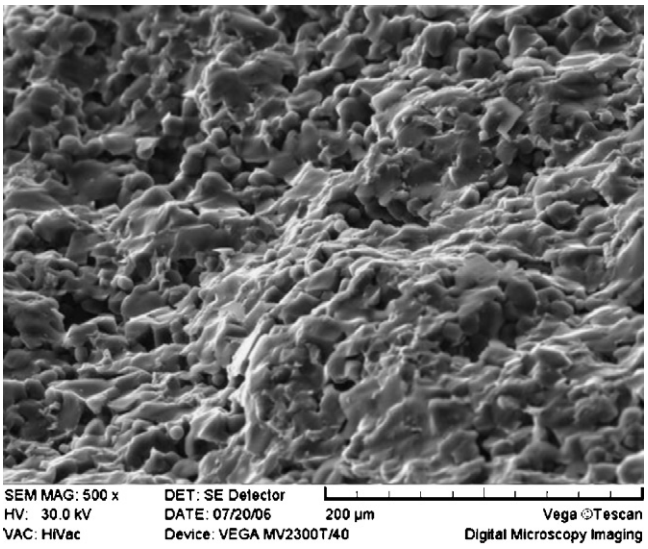

Fig. 6. Fractograph of $B_4C + 25\%$ ZrO_2 sample.

Microstructure of sample with 25% ZrO_2 is presented without etching (Fig. 5d).

Fractography of $B_4C + 25\%$ ZrO_2 sample is shown in Fig. 6. The picture shows clear cleavage planes and the mode of fracture to be a combination of transgranular and intergranular. The grain size appears to be in the range of 10–40 μm.

Optical images of samples sintered with ZrO_2 addition show the presence of second phase. XRD of the samples indicated the second phase to be that of ZrB_2which is in line with the reported literature. But the amount of the second phase appears to be more than the possible quantum. In order to confirm this, the samples were analysed By EPMA, where it was revealed that second phase contained Zr, B and Carbon. Quantitative analysis of the second phase revealed the presence of zirconium in the range of 1.17–1.24 wt.% only (Fig. 7). Our repeated EPMA analysis of this phase at various locations as well as different samples shows identical results. As XRD analysis of our samples is consistent with the reported literature, the second phase may be assumed to contain a small amount of tiny crystals of ZrB_2. As this is the first attempt to do quantitative elemental analysis of the second phase, further confirmation by TEM is needed to understand this phase properly. Back scattered image of the polished surface of the sample and line scan across the phases for Zr and boron are presented in Fig. 8. Presence of zirconium and a reduction in the quantity of boron could be seen in the white phase. Elemental mapping of the same sample for Zr and B are shown in Fig. 9. These pictures confirm the above observation.

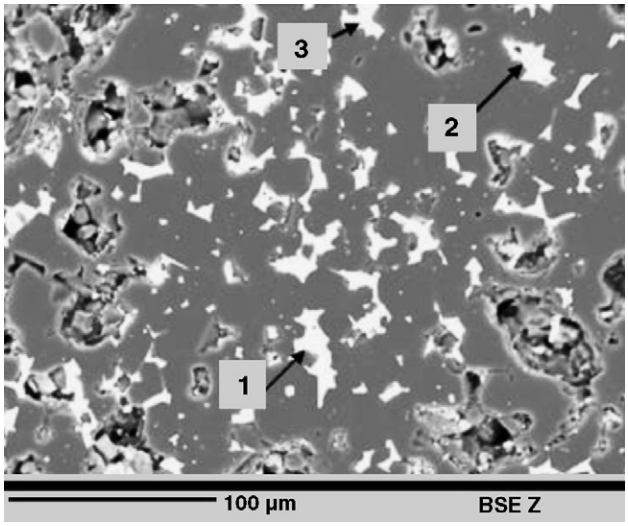

Fig. 7. Quantitative analysis of Zirconium at white phase. Spot 1, 1.24 wt.%; spot 2, 1.24 wt.%; spot 3, 1.17 wt.%.

3.6. Thermal conductivity

Thermal diffusivity of the samples in the temperature range of 400–1000 °C was measured using a LASERFLASH thermal diffusivity measuring system. The thermal diffusivity data was corrected for radiation losses and finite pulse width effects. Thermal conductivity (λ) was calculated using the following formula from thermal diffusivity

$$\lambda = \frac{k}{(\rho C_p)}$$

where k is the thermal conductivity, ρ is the geometrical density and C_p is the specific heat capacity. Specific heat of B_4C was measured using differential scanning calorimeter (SW 8.10 Mettler), and specific heat of the mixture of B_4C and ZrB_2 was calculated using Neumann–Kopp's molar additivity rule [19]. The specific heat data of ZrB_2 for the above calculation was taken from the literature [20,21].

Heat capacity of boron carbide with temperature in the range of 673–1473 K is shown in Fig. 10. These values are matching with those of Gilchrist and Preston [22]. Thermal diffusivity of

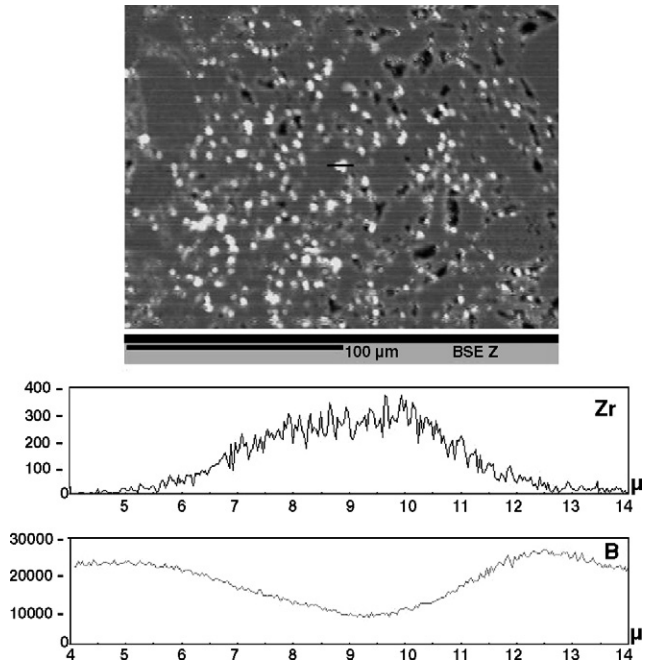

Fig. 8. Back scattered image of $B_4C + 7.5\%$ ZrO_2 sample and line scan across the white phase for Zr and B.

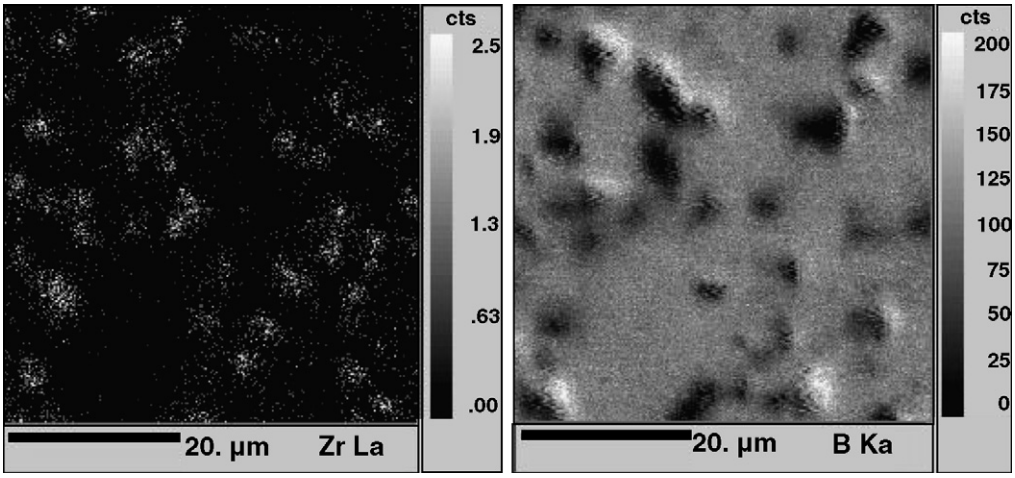

Fig. 9. Elemental mapping of B_4C + 7.5% ZrO_2 image for Zr and B.

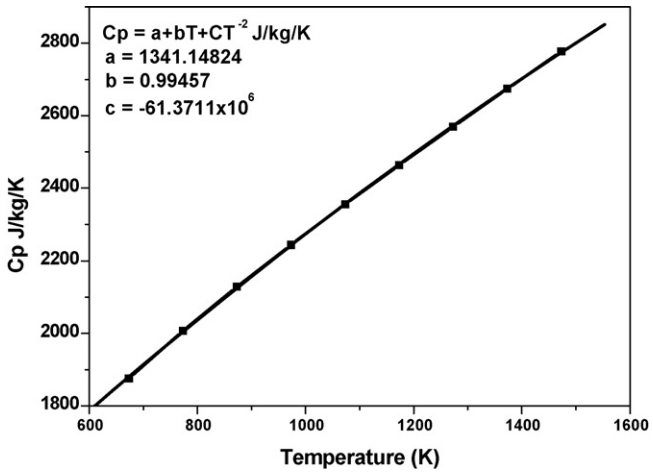

Fig. 10. Heat capacity of boron carbide with temperature.

B_4C and $B_4C + ZrO_2$ samples are presented in Fig. 11. Wood et al. have synthesized boron carbide with varying carbon content and measured thermal conductivities [23]. They have shown that thermal diffusivity of B_4C is much more sensitive to temperature compared to that of $B_{6.5}C$, $B_{7.5}C$ and B_9C. The thermal diffusivity values of our sample match with that of $B_{6.5}C$. The higher B/C ratio of our sample coupled with the presence of free carbon indicates the presence of larger amounts of $B_{6.5}C$ in our sample. Measured thermal diffusivity values also affirm this. Samples sintered with ZrO_2 showed marginally higher values of thermal diffusivity at all the temperatures. The temperature dependence also is very similar to that of 0% ZrO_2 sample. Thermal diffusivity of boron carbide–zirconium boride composite has not been reported in the literature.

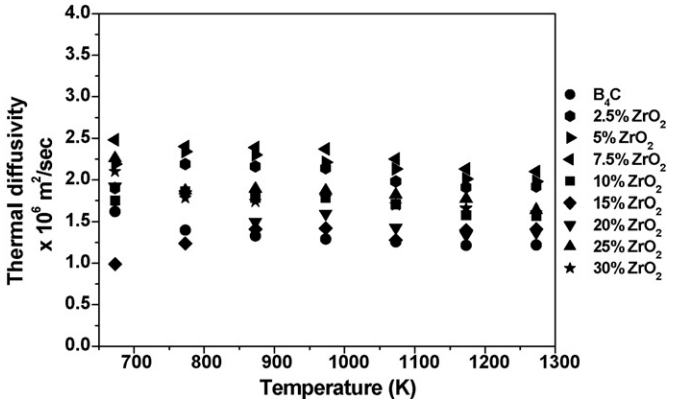

Fig. 11. Thermal diffusivity of boron carbide and $B_4C + ZrO_2$ composites as a function of temperature.

4. Conclusions

Addition of ZrO_2 while pressureless sintering of boron carbide was found to be beneficial in densification. Samples sintered at 2275 °C for 60 min with the addition of ≥5 wt.% ZrO_2 showed densities in the range of 93–96% ρth, compared to 86.63% ρth for B_4C only. Hardness of the samples sintered with ZrO_2 additive was found to be higher at 30–31.5 GPa, compared to 27 GPa of B_4C. XRD showed the presence of ZrB_2 in the sintered samples. Optical microscopy of the polished specimens showed the presence of second phase in the matrix. Fractography of sample with ZrO_2 exhibited mixed mode of fracture. Line scan and spot analysis by EPMA showed the presence of zirconium in the second phase. Thermal conductivity of the samples in the temperature range of 400–1000 °C was measured to be marginally higher values with the addition of ZrO_2.

References

[1] F. Thevnot, J. Eur. Ceram. Soc. 6 (1990) 205.
[2] D.E. Mahagin, R.E. Dahl, Nuclear applications of boron and the borides, in: V.I. Matkovich (Ed.), Boron and Refractory Borides, Springler-Verlag, New York, 1977, pp. 613–632.
[3] F. Thevenot, A review on boron carbide, Key Eng. Mater. 56–57 (1991) 59–88.
[4] R.F. Speyer, H. Lee, Advances in pressureless densification of boron carbide, J. Mater. Sci. 39 (2004) 6017–6021.
[5] A. Goldstein, Y. Geffen, A. Goldenberg, Boron carbide-Zirconium boride in situ composites by the reactive pressureless sintering of boron carbide-zirconia mixtures, J. Am. Ceram. Soc. 84 (3) (2001) 642–644.
[6] H.W. Kim, Y.H. Koh, H.E. Kim, J. Mater. Res. 15 (11) (2000) 2431–2436.

[7] L. Levin, N. Frage, M.P. Dariel, Metall. Mater. Trans. A 30A (1999) 3201–3210.
[8] L. Levin, N. Frage, M.P. Dariel, Int. J. Refract. Met. Hard Mater. 18 (2000) 131–135.
[9] V. Skorokhod Jr., M.D. Vlajic, V.D. Krstic, J. Mater. Sci. Lett. 15 (1996) 1337–1339.
[10] N. Frage, Effects of addition of chromium oxide on sintering of boron carbide, in: 15th International Plansee Seminar, Reutte, Austria, May, 2001.
[11] A. Golstein, Y. Yeshurun, A. Goldenberg, J. Euro. Ceram. Soc. 27 (2007) 695–700.
[12] L.S. Sigl, J. Euro. Ceram. Soc. 18 (1998) 1521–1529.
[13] N. Frage, L. Levin, M.P. Dariel, J. Solid Stage Chem. 177 (2004) 410–414.
[14] T.K. Roy, C. Subramanian, A.K. Suri, Ceram. Int. 32 (2006) 227–233.
[15] Etchants database version 2.0 copyright © 2004 by Henrik kaker.
[16] M. Bouchacourt, F. Thevenot, J. Less Common Met. 82 (1981) 219–226.
[17] K. Fromet, C. Chatillon, J. Fouletier, M. Fouletier, J. Nucl. Mater. 188 (1992) 280–284.
[18] D. Gosset, M. Colin, J. Nucl. Mater. 183 (1991) 161–173.
[19] C.H.P. Lupis, Chemical Thermodynamics of Materials, North-Holland, New York, 1983, p. 29.
[20] I. Barin, third ed., Thermochemical data of pure substances, vol. 2, VCH, Weinheim, 1995.
[21] O. Kubaschewski, C.B. Alcock, Metallurgical Thermodynamics, Pergamon, New York, 1979, p. 354.
[22] K.E. Gilchrist, S.D. Preston, High Temp. High Pres. 11 (1979) 643.
[23] C. Wood, D. Emin, P.E. Gray, Phys. Rev. B 31 (10) (1985) 6811–6814.